

Accurate measurement of the standard $^{235}\text{U}(n,f)$ cross section from thermal to 170 keV neutron energy

S. Amaducci^{15,35}, O. Aberle¹, J. Andrzejewski², L. Audouin³, M. Bacak^{4,1,5}, J. Balibrea⁶, M. Barbagallo⁷, F. Bečvář⁸, E. Berthoumieux⁵, J. Billowes⁹, D. Bosnar¹⁰, A. Brown¹¹, M. Caamaño¹², F. Calviño¹³, M. Calviani¹, D. Cano-Ott⁶, R. Cardella¹, A. Casanovas¹³, F. Cerutti¹, Y. H. Chen³, E. Chiaveri^{1,9,14}, N. Colonna⁷, G. Cortés¹³, M. A. Cortés-Giraldo¹⁴, L. Cosentino¹⁵, L. A. Damone^{7,16}, M. Diakaki⁵, C. Domingo-Pardo¹⁷, R. Dressler¹⁸, E. Dupont⁵, I. Durán¹², B. Fernández-Domínguez¹², A. Ferrari¹, P. Ferreira¹⁹, P. Finocchiaro¹⁵, V. Furman²⁰, K. Göbel²¹, A. R. García⁶, A. Gawlik², S. Gilardoni¹, T. Glodariu²², I. F. Gonçalves¹⁹, E. González-Romero⁶, E. Griesmayer⁴, C. Guerrero¹⁴, F. Gunsing^{5,1}, H. Harada²³, S. Heinitz¹⁸, J. Heyse²⁴, D. G. Jenkins¹¹, E. Jericha⁴, F. Käppeler²⁵, Y. Kadi¹, A. Kalamara²⁶, P. Kavargin⁴, A. Kimura²³, N. Kivel¹⁸, I. Knapova⁸, M. Kokkoris²⁶, M. Krtička⁸, D. Kurtulgil²¹, E. Leal-Cidoncha¹², C. Lederer²⁷, H. Leeb⁴, J. Lerendegui-Marco¹⁴, S. Lo Meo^{28,29}, S. J. Lonsdale²⁷, D. Macina¹, A. Manna^{29,30}, J. Marganiec^{2,31}, T. Martínez⁶, A. Masi¹, C. Massimi^{29,30}, P. Mastinu³², M. Mastromarco⁷, E. A. Mauger¹⁸, A. Mazzone^{7,33}, E. Mendoza⁶, A. Mengoni²⁸, P. M. Milazzo³⁴, F. Mingrone¹, A. Musumarra^{15,35}, A. Negret²², R. Nolte³¹, A. Oprea²², N. Patronis³⁶, A. Pavlik³⁷, J. Perkowski², I. Porras³⁸, J. Praena³⁸, J. M. Quesada¹⁴, D. Radeck³¹, T. Rauscher^{39,40}, R. Reifarth²¹, C. Rubbia¹, J. A. Ryan⁹, M. Sabaté-Gilarte^{1,14}, A. Saxena⁴¹, P. Schillebeeckx²⁴, D. Schumann¹⁸, P. Sedyshev²⁰, A. G. Smith⁹, N. V. Sosnin⁹, A. Stamatopoulos²⁶, G. Tagliente⁷, J. L. Tain¹⁷, A. Tarifeño-Saldivia¹³, L. Tassan-Got³, S. Valentá⁸, G. Vannini^{29,30}, V. Variale⁷, P. Vaz¹⁹, A. Ventura²⁹, V. Vlachoudis¹, R. Vlastou²⁶, A. Wallner⁴³, S. Warren⁹, C. Weiss⁴, P. J. Woods²⁷, T. Wright⁹, and P. Žugec^{10,1}
and the n_TOF Collaboration

¹European Organization for Nuclear Research (CERN), Switzerland

²University of Lodz, Poland

³Institut de Physique Nucléaire, CNRS-IN2P3, Univ. Paris-Sud, Université Paris-Saclay, F-91406 Orsay Cedex, France

⁴Technische Universität Wien, Austria

⁵CEA Irfu, Université Paris-Saclay, F-91191 Gif-sur-Yvette, France

⁶Centro de Investigaciones Energéticas Medioambientales y Tecnológicas (CIEMAT), Spain

⁷Istituto Nazionale di Fisica Nucleare, Sezione di Bari, Italy

⁸Charles University, Prague, Czech Republic

⁹University of Manchester, United Kingdom

¹⁰Department of Physics, Faculty of Science, University of Zagreb, Zagreb, Croatia

¹¹University of York, United Kingdom

¹²University of Santiago de Compostela, Spain

¹³Universitat Politècnica de Catalunya, Spain

¹⁴Universidad de Sevilla, Spain

¹⁵INFN Laboratori Nazionali del Sud, Catania, Italy

¹⁶Dipartimento di Fisica, Università degli Studi di Bari, Italy

¹⁷Instituto de Física Corpuscular, CSIC - Universidad de Valencia, Spain

¹⁸Paul Scherrer Institut (PSI), Villigen, Switzerland

¹⁹Instituto Superior Técnico, Lisbon, Portugal

²⁰Joint Institute for Nuclear Research (JINR), Dubna, Russia

²¹Goethe University Frankfurt, Germany

²²Horia Hulubei National Institute of Physics and Nuclear Engineering, Romania

²³Japan Atomic Energy Agency (JAEA), Tokai-mura, Japan

²⁴European Commission, Joint Research Centre, Geel, Retieseweg 111, B-2440 Geel, Belgium

²⁵Karlsruhe Institute of Technology, Campus North, IKP, 76021 Karlsruhe, Germany

²⁶National Technical University of Athens, Greece

²⁷School of Physics and Astronomy, University of Edinburgh, United Kingdom

²⁸Agenzia nazionale per le nuove tecnologie (ENEA), Bologna, Italy

²⁹Istituto Nazionale di Fisica Nucleare, Sezione di Bologna, Italy

³⁰Dipartimento di Fisica e Astronomia, Università di Bologna, Italy

³¹Physikalisch-Technische Bundesanstalt (PTB), Bundesallee 100, 38116 Braunschweig, Germany

³²Istituto Nazionale di Fisica Nucleare, Sezione di Legnaro, Italy

³³Consiglio Nazionale delle Ricerche, Bari, Italy

³⁴Istituto Nazionale di Fisica Nucleare, Sezione di Trieste, Italy

³⁵Dipartimento di Fisica e Astronomia, Università di Catania, Italy

³⁶University of Ioannina, Greece

³⁷University of Vienna, Faculty of Physics, Vienna, Austria

³⁸University of Granada, Spain

³⁹Department of Physics, University of Basel, Switzerland

⁴⁰Centre for Astrophysics Research, University of Hertfordshire, United Kingdom

⁴¹Bhabha Atomic Research Centre (BARC), India

⁴²Istituto Nazionale di Fisica Nucleare, Sezione di Perugia, Italy

⁴³Australian National University, Canberra, Australia

Abstract.

An accurate measurement of the $^{235}\text{U}(n,f)$ cross section from thermal to 170 keV of neutron energy has recently been performed at n_TOF facility at CERN using $^6\text{Li}(n,t)^4\text{He}$ and $^{10}\text{B}(n,\alpha)^7\text{Li}$ as references. This measurement has been carried out in order to investigate a possible overestimation of the ^{235}U fission cross section evaluation provided by most recent libraries between 10 and 30 keV. A custom experimental apparatus based on in-beam silicon detectors has been used, and a Monte Carlo simulation in GEANT4 has been employed to characterize the setup and calculate detectors efficiency. The results evidenced the presence of an overestimation in the interval between 9 and 18 keV and the new data may be used to decrease the uncertainty of $^{235}\text{U}(n,f)$ cross section in the keV region.

1 Introduction

Most of the neutron cross sections are measured using a standard reaction as reference, i.e. a small group of reactions known with high accuracy in a well defined energy interval [1] [2]. The use of this reference implies that the knowledge of the standard determines the achievable accuracy on the measured cross section. The $^{235}\text{U}(n,f)$ is one of the most used references, thanks to the wide neutron energy range, indeed it is defined as standard at thermal (0.0253 eV) and from 0.15 to 200 MeV.

Recent experimental data [3] highlighted a possible overestimation of the ^{235}U fission cross section in the major libraries in the neutron energy range between 10 and 30 keV. Even if in this interval the $^{235}\text{U}(n,f)$ is not a standard, it is still often used as reference, in particular for capture and fission cross section measurements of actinides. This energy interval is interesting for many technological applications, in particular for the design of new generation fission reactors and for nuclear waste burning, which require accurate neutron cross section data.

In 2016 at n_TOF facility a new measurement of the $^{235}\text{U}(n,f)$ cross section was performed, in order to obtain accurate data and investigate further on this discrepancy. For this measurement two different standard reactions have been used as references, namely $^6\text{Li}(n,t)^4\text{He}$ and $^{10}\text{B}(n,\alpha)^7\text{Li}$, while a stack of in-beam silicon detectors has been used to detect the reaction products. Even though in-beam silicon detectors have already been employed at n_TOF (see ref. [4]), this was the first time that in-beam silicon detectors were used to measure fission reactions at n_TOF.

2 Experimental setup

The measurement has been performed in the first experimental area of n_TOF facility at CERN. At n_TOF the protons accelerated by the PS (Proton Synchrotron) interact with a lead target and produce through a spallation process a pulsed neutron beam characterized by a very high instantaneous flux, this feature comes to prove to be very

useful to increase the signal-to-background ratio when the sample is radioactive like the ^{235}U . The neutron energy is measured using the time of flight technique with a resolution of 10^{-3} - 10^{-4} , thanks to the long flight path (around 185 m).

The $^{235}\text{U}(n,f)$ cross section has been measured using $^6\text{Li}(n,t)$ and $^{10}\text{B}(n,\alpha)$ as reference, single pad silicon detectors were used to measure the reaction products, taking advantage of their good energy resolution to discriminate the products from the background. Six silicon and six samples have been arranged so that each detector faces only one sample as it is reported in fig. 1, the apparatus was placed in-beam and the neutrons were crossing all the detectors and samples. The silicon detectors were 200 μm thick, ensuring all the particles were stopped inside the detectors, and having an area of $5 \times 5 \text{ cm}^2$, relaxes the alignment constraint since the area is large compared to the n_TOF beam dimensions. For each reaction two detectors have been used, one placed after the corresponding sample, in order to measure the products in the forward direction with respect to the neutron beam, and one before the target to cover the backward direction. The presence of two detectors increases the redundancy and compensates to a large extent the systematic uncertainty due to angular anisotropy emission of products.

3 Data analysis

A calibration of the flight path has been performed with a linear fit of the first resonances of the $^{235}\text{U}(n,f)$, followed by a minimization of χ^2 between experimental data and ENDF-B/VIII evaluation, the value of $L = 183.49(2) \text{ m}$ has been later used to transform the time of flight into kinetic energy. Thanks to the design of the experimental apparatus all the target samples shared the same neutron flux, apart from a correction due to absorption in the materials along the beam. Moreover the samples were thin enough to apply the thin-target approximation and the $^{235}\text{U}(n,f)$ cross section can be calculated from the equation:

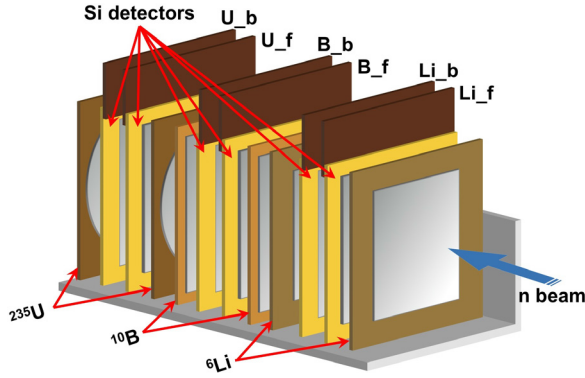


Figure 1. Design of the experimental apparatus, the silicons are named after the coupled sample, with the suffix "_f" for the forward direction and "_b" for the backward one.

$$\sigma_{235U} = \frac{C_{235U} f_{ref} \rho_{ref} \epsilon_{ref}}{C_{ref} f_{235U} \rho_{235U} \epsilon_{235U}} \sigma_{ref} \quad (1)$$

where *ref* indicates a generic reference reaction. In eq. 1 C_X is the count rate with respect to the neutron energy, f_X is the correction for the absorption in the materials crossed, ϵ_X is the efficiency and ρ_X is the areal density. The count rate is obtained selecting the reaction products with a experimental threshold on the deposited energy, in particular for the reaction ${}^6\text{Li}(n,t)$ we selected the tritons, for ${}^{10}\text{B}(n,\alpha)$ the alphas and for ${}^{235}\text{U}(n,f)$ the fission fragments. The top panel of fig. 2 shows the two dimensional matrix of signal amplitude versus neutron energy for the silicon coupled with ${}^{235}\text{U}$ sample, together with the threshold used to select the fission fragments. The wide separation between the alpha particles and the fragments is clear. The bottom panel shows the amplitude spectra of the same detector for different neutron energy intervals, on the right-hand side one can identify the two-peak structure resulting from the asymmetric fission of ${}^{235}\text{U}$, the spectra are compressed due to a logarithmic behavior of the preamplifier for deposited energy larger than 10 MeV.

The full experimental apparatus has been implemented in a Monte Carlo simulation made with the GEANT4 [6] code, in order to evaluate the correction factor for the absorption f_X and the efficiencies of ${}^6\text{Li}(n,t)$ and ${}^{10}\text{B}(n,\alpha)$. For the absorption a neutron beam with the same shape of the n_TOF one was simulated, the correction is represented by the fraction of neutrons entering in each target sample with respect to the simulated ones. The correction is mainly determined by the large cross section of ${}^6\text{Li}$ and ${}^{10}\text{B}$ at thermal and by the aluminum that composes the samples bakings and has large capture resonances in the keV region. The simulation was employed as well to calculate the efficiency of ${}^6\text{Li}(n,t)$ and ${}^{10}\text{B}(n,\alpha)$, since for both these reactions the efficiency depends on neutron energy, in particular the main dependence is due to the anisotropy in the emission in the keV region. The reactions have been simulated according to the product angular distribution provided by ENDF-B/VIII [7], of course the experimental threshold has been calibrated and included in the simulation. The efficiency of the fission reaction

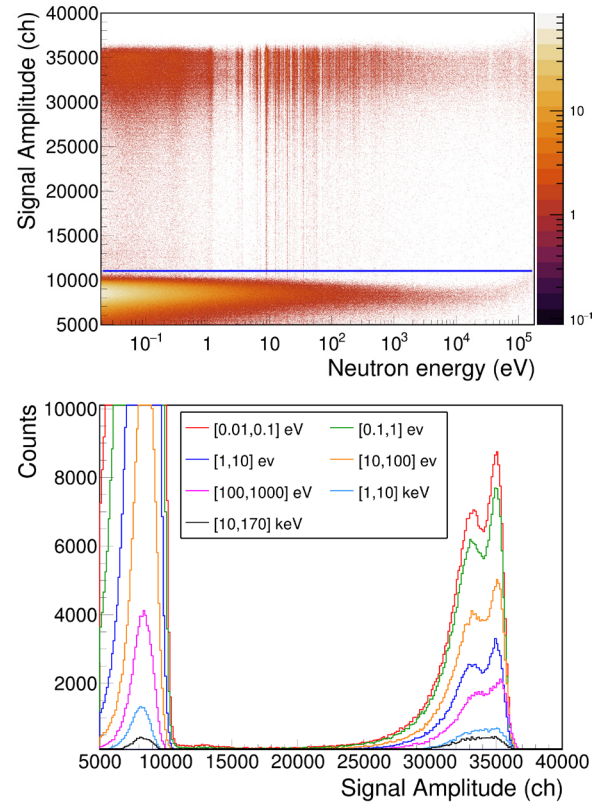


Figure 2. Top panel: two dimensional plot of signals amplitude versus neutron energy for a silicon coupled to a ${}^{235}\text{U}$ sample, the blue threshold separates fission fragments (upper region) from alpha particles (lower region). Bottom panel: amplitude spectra of the same detector for different neutron energy intervals, the separation of FF (right side) from the alpha background (left side) is very well defined.

can be considered constant at this energy, thanks to the large Q-value (around 200 MeV) and the isotropic angular emission of fragments. Further details about the GEANT4 simulations are presented in ref. [8]. Once the corrections for absorption and efficiency have been applied for each reaction, the data of forward and backward detectors have been combined with a weighted average.

After all the quantities that depend on the neutron energy have been calculated the shape of the fission cross section is obtained from eq. 1, apart from a constant term that includes the areal densities and the fission detection efficiency. This term has been calculated by normalizing the data to the integral of the ${}^{235}\text{U}(n,f)$ cross section between 7.8 and 11 eV as recommended by ref. [1], since in this interval between two cross section minima the uncertainty arising from the time-to-energy calibration is negligible. Moreover at this energy the absorption is small and the contribution to the uncertainty coming from the correction is small.

Table 1 lists the ratio between the thermal point, where the ${}^{235}\text{U}(n,f)$ is a standard, and the integral between 7.8 and 11 eV for the IAEA and the measured cross section with the two standard references. The agreement is within 1 standard deviation, making the choice of the normaliza-

	Ratio $\sigma_{th} / \text{integral}[7.8,11]\text{eV} (\text{eV}^{-1})$
IAEA2018	2.373 ± 0.029
${}^6\text{Li}$ as ref.	$2.353 \pm 0.013(\text{stat}) \pm 0.007(\text{syst})$
${}^{10}\text{B}$ as ref.	$2.343 \pm 0.019(\text{stat}) \pm 0.007(\text{syst})$
${}^{10}\text{B}+{}^6\text{Li}$	$2.352 \pm 0.013(\text{stat}) \pm 0.007(\text{syst})$

Table 1. Ratio between thermal and the [7.8,11]eV integral for IAEA and the experimental cross section measured with two standard reference reactions.

tion in the 7.8 to 11 eV interval consistent with thermal standard point. Finally a final n_{TOF} ${}^{235}\text{U}(n,f)$ cross section is calculated combining the two references ${}^6\text{Li}(n,t)$ and ${}^{10}\text{B}(n,\alpha)$ through a weighted average.

4 Results

The measured ${}^{235}\text{U}(n,f)$ cross section calculated with the two standard reactions ${}^6\text{Li}(n,t)$ and ${}^{10}\text{B}(n,\alpha)$ has been compared with ENDF-B/VIII [7], JEFF3.3 [9], JENDL4.0 [10] and IAEA [1] in the integrals reported in fig. 3. The top panel reports the ratio between the n_{TOF} fission cross section integral and the libraries, while the bottom panel presents the deviation in standard deviation units. In the first integral considered the measured cross section is 4-5% lower than all the libraries with the exception of JENDL4.0, for the first three libraries this deviation is statistically significant, however this deviation is absent in the integral from 18 to 30 keV, where the ratio is compatible with 1. The resulting effect on the 9 to 30 keV integral is a smaller deviation, indeed it is approximately 2%, even in terms of standard deviation the discrepancy is not significant, since the difference is lower than 3σ with respect to all the considered libraries. On the opposite the new data are in good agreement with JENDL4.0 for all the considered integrals, with deviations around or smaller than 1σ . The reliability of the present result is guaranteed by the good agreement in the energy regions where the ${}^{235}\text{U}(n,f)$ is a standard, in particular the differences between 150 and 170 keV are lower than 1% and the agreement at thermal is evidenced in tab. 1.

It is important to note that the IAEA values in this energy range are reported in form of point-wise cross section and the IAEA cross section of fig. 3 is calculated by applying a linear interpolation as recommended by ref. [1]. For ENDF-B/VIII, JEFF3.3 and JENDL4.0 there is no appreciable effect arising from interpolation, thanks to the narrow energy interval between two consecutive points. In order to make a direct comparison, removing the effects due to the interpolation procedure, the experimental data have been adapted to the IAEA energy grid. Later the ${}^{235}\text{U}(n,f)$ cross section measured with ${}^6\text{Li}(n,t)$ and ${}^{10}\text{B}(n,\alpha)$ has separately been compared with IAEA values. The resulting ratios between the experimental data and IAEA values are reported in fig. 4 for the two separate data-sets, one can note that the deviation in the 9 to 18 keV integral previously discussed arises from the large difference (about 7%) for the point at 9.5 keV. However with the exception of the

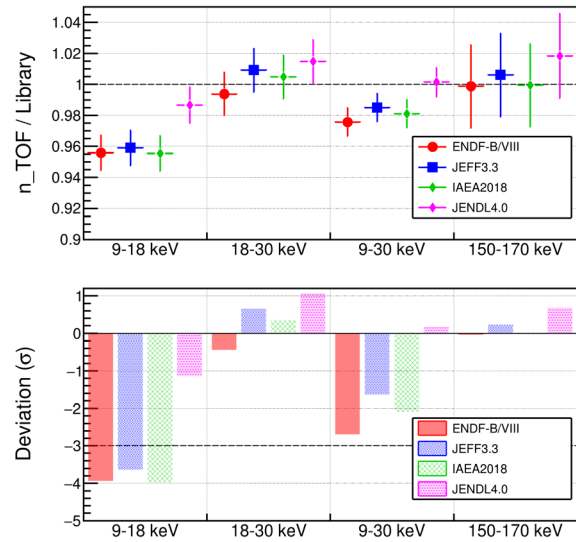


Figure 3. Comparison between n_{TOF} measured cross section and the values of more recent libraries integrated on intervals of interest.

point at 9.5 keV the experimental data are in agreement with the IAEA values.

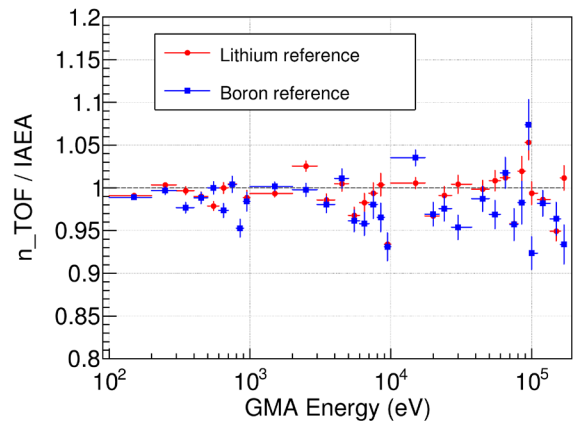


Figure 4. Ratio between measured cross section and the IAEA in correspondence of GMA nodes.

5 Conclusion

The ${}^{235}\text{U}(n,f)$ is one of the most used standard cross section and the evidences of an overestimation between 10 and 30 keV in major libraries required further investigations. An accurate measurement of the ${}^{235}\text{U}$ fission cross section has been performed at n_{TOF} from thermal to 170 keV neutron energy, using the standard reactions ${}^6\text{Li}(n,t)$ and ${}^{10}\text{B}(n,\alpha)$ as references and employing a custom experimental apparatus based on in-beam silicon detectors. The experimental setup and the data analysis are described in more detail in the complete article in ref. [8], the final data sets are available on EXFOR (23453.).

The results highlighted an overall discrepancy between experimental data and three of the four considered libraries

around 2% in the energy interval 9 to 30 keV, this difference resulted to be smaller than what has been observed in ref. [3]. In the energy region between 9 and 18 keV we found an overestimation around 4-5% in comparison to the evaluated cross section by ENDF-B/VIII, JEFF3.3 and IAEA. On the contrary no significant deviations have been observed between 18 and 30 keV for the mentioned libraries.

Since the IAEA cross section is calculated through an interpolation of point-wise values, the n_TOF experimental data have been adapted to the IAEA grid and a direct comparison point-by-point has been done. The cross sections measured with the two references, namely ${}^6\text{Li}(n,t)$ and ${}^{10}\text{B}(n,\alpha)$, have been separately compared with the IAEA points. The experimental values are in a good agreement with the exception of the point at 9.5 keV, where a difference of the 7% has been observed. Indeed the discrepancy observed in the energy interval from 9 to 18 keV is due to this large difference in a single point together with the use of a linear interpolation.

The reliability of these experimental data is assured by the good agreement in the energy interval where the ${}^{235}\text{U}(n,f)$ cross section is a standard, namely at thermal energy and from 150 to 170 keV. The new data available

may be used to reduce uncertainty on the ${}^{235}\text{U}(n,f)$ cross section, in particular concerning the keV region. Furthermore this may lead in future to move the lower limit of the interval where the ${}^{235}\text{U}(n,f)$ is a standard, at present 150 keV, to lower energies.

References

- [1] A.D. Carlson et al., Nucl. Data Sheets **148** 143-188 (2018)
- [2] A.D. Carlson et al., Nucl. Data Sheets **110** 3215 (2009)
- [3] M. Barbagallo et al., Eur. Phys. J. A **49** 156 (2013)
- [4] L. Cosentino et al., Nucl. Instrum. Methods A **830** 197 (2016)
- [5] C. Guerrero et al., Eur. Phys. J. A **49** 27 (2013)
- [6] S. Agostinelli et al., Nucl. Instrum. Methods Phys. Res. A **506** 250 (2003)
- [7] D. A. Brown et al., Nucl. Data Sheets **148** 1 (2018)
- [8] S. Amaducci et al., Eur. Phys. J. A **55** 120 (2019)
- [9] <https://www.oecd-nea.org/dbdata/jeff/jeff33/>
- [10] K. Shibata et al., J. Nucl. Sci. Technol. **48** 1 (2011)